

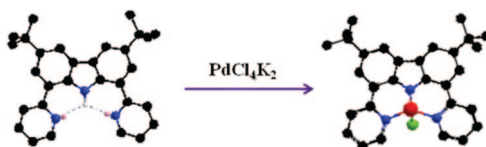
Preparation and Study of 1,8-Di(pyrid-2'-yl)carbazoles

Maria S. Mudadu, Ajay N. Singh, and Randolph P. Thummel*

Department of Chemistry, 136 Fleming Building, University of Houston, Houston, Texas 77204-5003

thummel@uh.edu

Received August 15, 2007



A series of three derivatives of 1,8-di(pyrid-2'-yl)carbazole were prepared by Stille-type coupling of 2-(tri-*n*-butylstannyl)pyridine with the appropriate 1,8-dibromocarbazole. The carbazoles were prepared by appropriate substitution methodologies on the parent carbazole or by palladium-catalyzed cyclization of di-(*p*-tolyl)amine to provide the carbazole ring system. An X-ray structure of the di-*tert*-butyl derivative confirmed that both pyridyl groups were oriented for favorable intramolecular H-bonding to the central N–H. Two orientations of the molecule were found in the unit cell and this observation was corroborated by two N–H stretching bands in the solid state IR. Substitution of N–H by N–D led to increased emission intensity through diminished intramolecular deactivation of the excited state. The di-*tert*-butyl derivative formed a tridentate complex with Pd(II), which showed a red-shifted band attributed to an intraligand charge transfer state.

Introduction

The juxtaposition of pyridine and indole brings together two important fundamental aromatic nuclei with interesting complementary properties. The pyridine molecule is somewhat electron deficient but is nevertheless a good Lewis base due to the availability of the nitrogen lone pair electrons. It behaves as an important ligand and participates readily as an H-bond acceptor. The indole molecule is comparatively electron rich but only binds metals in its deprotonated form. It is highly fluorescent and behaves as a good H-bond donor.

In earlier work we have carefully examined the consequences of appending a pyridyl group to indole, either through the 2-indole¹ or 7-indole position.² For 2-(pyrid-2'-yl)indole (**1**) we found evidence for excited state proton transfer (ESPT) promoted by a cyclic H-bonded alcohol complex to provide an unstable tautomer with greatly diminished fluorescence.³ On the other hand, 7-(pyrid-2'-yl)indole (**2**) exhibits strong intramolecular H-bonding in the ground state, which leads to very

efficient ESPT to provide the tautomer **2b** and almost complete quenching of the excited state emission⁴ (Figure 1).

Carbazole represents a simple, symmetrical benzalogue of indole that can serve to amplify the intramolecular H-bonding characteristics of **2**. To further investigate this interesting system we have prepared the parent 1,8-di(pyrid-2'-yl)carbazole (**3H**) as well as the 3,6-dimethyl (**4H**) and 3,6-di-*tert*-butyl (**5H**) derivatives. The synthesis, structure, and properties of these systems will be presented along with some preliminary coordination chemistry.

Results and Discussion

Synthesis and Structure. The three carbazoles **3H–5H** were all prepared in the indicated yields by the Stille coupling of the

(1) (a) Thummel, R. P.; Hegde, V. *J. Org. Chem.* **1989**, *54*, 1720–1725. (b) Wu, F.; Hardesty, J.; Thummel, R. P. *J. Org. Chem.* **1998**, *63*, 4055–4061. (c) Wu, F.; Chamchoumis, C. M.; Thummel, R. P. *Inorg. Chem.* **2000**, *39*, 584–590.

(2) Mudadu, M. S.; Singh, A.; Thummel, R. P. *J. Org. Chem.* **2006**, *71*, 7611–7617.

(3) (a) Kyrychenko, A.; Herbich, J.; Wu, F.; Thummel, R. P.; Waluk, J. *J. Am. Chem. Soc.* **2000**, *122*, 2818–2827. (b) Herbich, J.; Hung, C.; Thummel, R. P.; Waluk, J. *J. Am. Chem. Soc.* **1996**, *118*, 3508–3518. (c) Herbich, J.; Hung, C.; Thummel, R. P.; Waluk, J. *J. Photochem. Photobiol. A: Chem.* **1994**, *80*, 157–160. (d) Kyrychenko, A.; Herbich, J.; Izydorczak, M.; Gil, M.; Dobkowski, J.; Wu, F.; Thummel, R. P.; Waluk, J. *Isr. J. Chem.* **1999**, *39*, 309–318. (e) Nosenko, Y.; Thummel, R. P.; Mordzinski, A. *Phys. Chem. Chem. Phys.* **2004**, *6*, 363–367.

(4) Wiosna, G.; Petkova, I.; Mudadu, M. S.; Thummel, R. P.; Waluk, J. *Chem. Phys. Lett.* **2004**, *400*, 379–383.

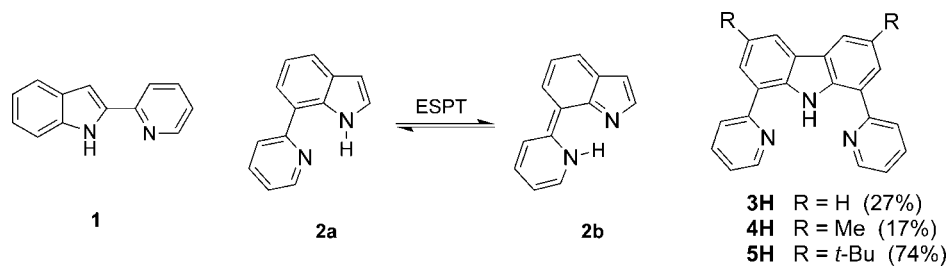
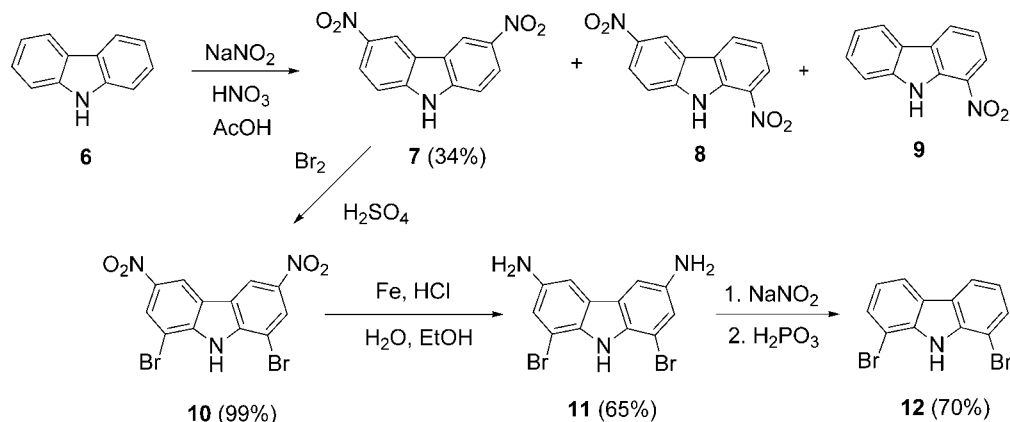
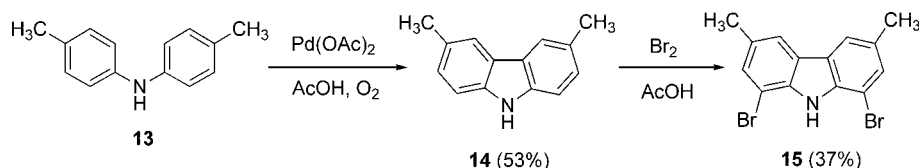


FIGURE 1. Relative orientation of pyridine and indole subunits in 1–5.

SCHEME 1



SCHEME 2



corresponding 1,8-dibromo derivatives with 2-(tri-*n*-butylstannyl)pyridine.⁵ Interestingly the dibromo derivatives were all made by significantly different approaches. To direct bromination exclusively to the 1,8-positions, one must first incorporate nitro groups at the 3,6-positions of carbazole (Scheme 1). Nitration of carbazole⁶ with sodium nitrite and nitric acid leads to a mixture of 1-nitro-, 1,6-dinitro-, and 3,6-dinitrocarbazoles (7–9) from which the desired 3,6-isomer could be isolated by chromatography in 34% yield. The bromination of 7 in sulfuric acid affords a nearly quantitative yield of the dibromo-derivative 10,⁷ which is then reduced with iron to the diamine in 65% yield. Finally the amine groups are diazotized in the normal fashion and removed with hypophosphorous acid to afford 12.⁸

Preparation of the dimethyl derivative followed a completely different approach, starting with di(*p*-tolyl)amine (13), which was oxidatively cyclized to provide 3,6-dimethylcarbazole (14) (Scheme 2). Initial attempts involved benzoyl peroxide in chloroform in the presence of light⁹ but this reaction results only in the recovery of the starting material. Rather, the

cyclization of 13 was performed with 1 equiv of palladium(II) diacetate in refluxing AcOH for 2 h.¹⁰ Several attempts to improve the reaction conditions always provided a 1:1 mixture of 13 and 14 which are difficult to separate. The incomplete cyclization of 13 can be attributed to a lack of oxidant in the mixture when the process is carried out under Ar. Moreover, recrystallized Pd(II) acetate and freshly distilled AcOH play an important role in the success of this reaction. When the cyclization is carried out in the presence of atmospheric oxygen, carbazole 14 is obtained pure in 53% yield.¹¹ This material was then brominated to give the dibromodimethyl derivative 15 in 37% yield.¹²

The *tert*-butyl analogue of 13 is less accessible so we once again started with the parent carbazole. Treatment with 4 equiv of *tert*-butyl chloride under Friedel–Crafts conditions resulted in a mixture of di-, tri-, and tetra-*tert*-butyl-substituted derivatives, with the more reactive 3,6-positions being substituted in

(10) Åkermark, B.; Ebersson, L.; Jonsson, E.; Pettersson, E. *J. Org. Chem.* **1975**, *40*, 1365–1367.

(11) (a) Watanabe, T.; Ueda, S.; Inuki, S.; Oishi, S.; Fujii, N.; Ohno, H. *Chem. Commun.* **2007**, 4516–4518. (b) Hagelin, H.; Oslob, J. D.; Åkermark, B. *Chem.–Eur. J.* **1999**, *5*, 2413–2416. (c) Åkermark, B.; Oslob, J. D.; Heuschert, U. *Tetrahedron Lett.* **1995**, *36*, 1325–1326.

(12) (a) Britovsek, G. J. P.; Gibson, V. C.; Hoarau, O. D.; Spitzmesser, S. K.; White, A. J. P.; Williams, D. J. *Inorg. Chem.* **2003**, *42*, 3454–3465. (b) Piatek, P.; Lynch, V. M.; Sessler, J. L. *J. Am. Chem. Soc.* **2004**, *126*, 16073–16076. (c) Coombs, N. D.; Stasch, A.; Cowley, A.; Thompson, A. L.; Aldridge, S. *Dalton Trans.* **2008**, 332–337. (d) Spitzmesser, S. K.; Gibson, V. C. *J. Organomet. Chem.* **2003**, *673*, 95–101. (e) Wentrup, C.; Gaugaz, M. *Helv. Chim. Acta* **1971**, *54*, 2108–2111.

(5) Schubert, U. S.; Eschbaumer, C.; Heller, M. *Org. Lett.* **2000**, *2*, 3373–3376.

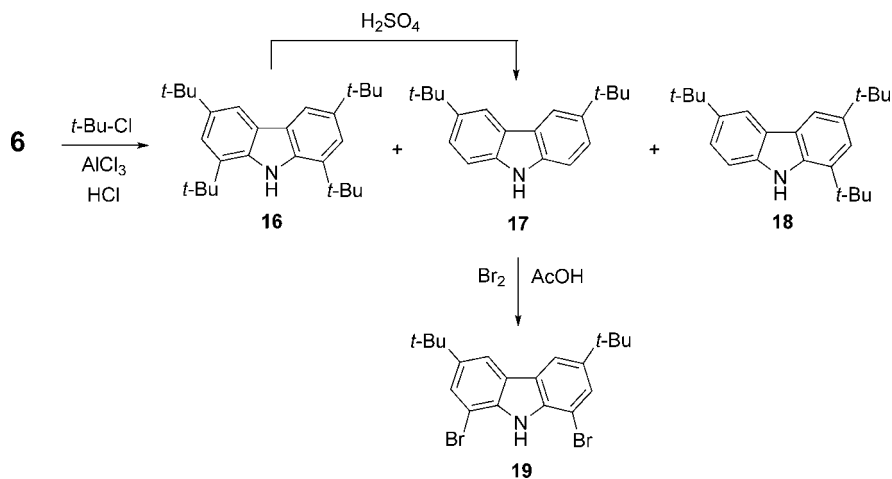
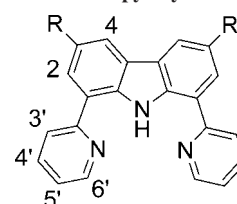
(6) Grotta, H. M.; Riggle, C. J.; Bearn, A. E. *J. Org. Chem.* **1964**, *29*, 2474–2476.

(7) Pieters, R. J.; Rebek, J. J. *Recl. Trav. Chim. Pays-Bas* **1993**, *112*, 330–334.

(8) (a) Kornblum, N. *Org. Synth.* **1955**, 295–299, Collect. Vol. III. (b) Suzuki, T.; Kinoshita, A.; Kawada, H.; Nakada, M. *Synlett.* **2003**, *4*, 570–572.

(9) Bhattacharyya, P.; Jash, S. S.; Dey, A. K. *J. Chem. Soc., Chem. Commun.* **1984**, 1668–1669.

SCHEME 3

TABLE 1. ^1H NMR Data for Dipyrindylcarbazoles^a


compd	H2	H3	H4	H3'	H4'	H5'	H6'
3H	8.06	7.35	8.00	8.22	7.85	7.30	8.93
4H	7.96		7.78	8.02	7.81	7.25	8.89
5H	8.23		8.02	8.05	7.86	7.28	8.90
20	8.27		7.92	8.22	7.92	7.26	10.14

^a Recorded in CDCl_3 at room temperature.

all three products¹³ (Scheme 3). These isomers could be separated efficiently by chromatography on silica gel. Interestingly, the tetra-*tert*-butyl isomer **16** could be dealkylated at the 1,8-positions to afford additional **17** in 58% yield. Finally, bromination of this material afforded **19** in 77% yield.¹⁴

The final Stille couplings of the dibromo precursors **12**, **15**, and **19** with 2-(tri-*n*-butylstannyl)pyridine were all accomplished in a similar manner with use of tetrakis(triphenylphosphine)-palladium(0) as the catalyst. Purification was accomplished by a combination of chromatography and recrystallization and the yields of the obtained carbazoles are given in Figure 1.

The carbazoles were all identified by their characteristic ^1H NMR spectra and these data are summarized in Table 1. The H6' proton exhibits a small coupling constant ($J_{\text{HH}} = 3.2\text{--}4.2$ Hz) and is always the lowest field signal, being strongly deshielded by the adjacent nitrogen. The remaining protons in the pyridine ring can be assigned by connectivity to H6'. The signals for H2 and H4 on the carbazole ring might be easily confused. We have assigned the more downfield signal to H2, which may experience greater deshielding due to proximity to N1' in conformations having the pyridine nitrogen pointing outward.

The 3,6-di-*tert*-butylcarbazole (**5H**) was further characterized by an X-ray crystal structure. The unit cell consists of two independent molecules (types A and B) which differ significantly

TABLE 2. Selected Geometric Parameters from the X-ray Structure of **5H**

Bond Lengths (Å)			
molecule A		molecule B	
C6–C7	1.481(4)	C39–C40	1.481
C11–C12	1.449(3)	C44–C45	1.448(3)
C16–C17	1.482(3)	C49–C50	1.482(4)
Dihedral Angles (deg)			
molecule A		molecule B	
C5–C6–C7–C8	–10.8(4)	N34–C39–C40–C58	18.0(4)
N1–C6–C7–C25	–11.4(4)	C38–C39–C40–C41	18.1(4)
C15–C16–C17–C18	–7.3(4)	C48–C49–C50–C51	–23.2(4)
C23–C16–C17–N22	–8.3(3)	C56–C49–C50–N55	–22.3(3)
Hydrogen Bonds (D–H...A)			
	D–H (Å)	H...A (Å)	∠DHA (deg)
molecule A			
N24–H1–N1	0.90(3)	2.28(3)	114(2)
N24–H1–N22	0.90(3)	2.17(3)	120(2)
molecule B			
N57–H34–N34	0.88(3)	2.26(3)	120(2)
N57–H34–N55	0.88(3)	2.33(3)	114(3)

in their arrangement and the torsional twist of the pyridine rings. This difference seems to be due solely to crystal packing forces. The *tert*-butyl groups in both molecules are disordered. An ORTEP plot of the type A molecule is given in Figure 2 along with the atomic numbering scheme for both type A and type B molecules. Table 2 summarizes some pertinent geometric data.

The different arrangements of two molecules of type A and two molecules of type B are shown in Figure 3. In the center of the unit cell, there are two molecules of type A, which are almost flat and parallel to each other. For molecule A, the torsion angles around the bond connecting the pyridine and carbazole rings, 11.1° for C(6)–C(7) and 7.8° for C(16)–C(17), are taken as the average of the two dihedral angles associated with the inter-ring bond. The two carbazole units are oriented in opposite directions and the pyridines partially overlap each other in a staggered manner. The molecules of type B surround the central type A molecules and are found at the edges of the unit cell. The type A molecules are paired and each molecule of every pair overlaps with half of the type B molecule. In particular, one pyridine lies on the top of the carbazole of the type B molecule. For the type B molecule, the *tert*-butyl group of one of the pair is situated between the pyridine rings of the other

(13) Neugebauer, F. A.; Fischer, H. *Chem. Ber.* **1972**, *105*, 2686–2693.(14) Gibson, V. C.; Spitzmesser, S. K.; White, A. J. P.; Williams, D. J. *Dalton Trans.* **2003**, 2718–2727.

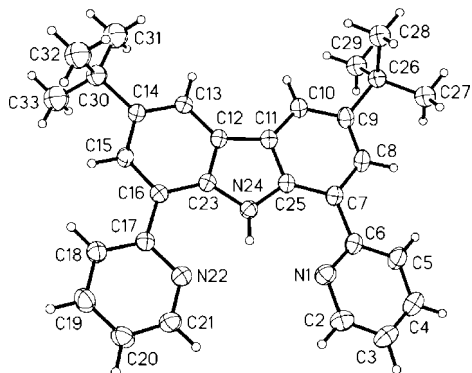


FIGURE 2. ORTEP plot of the type A molecule of **5H** with atom numbering scheme. Add +33 for numbering of the type B molecule.

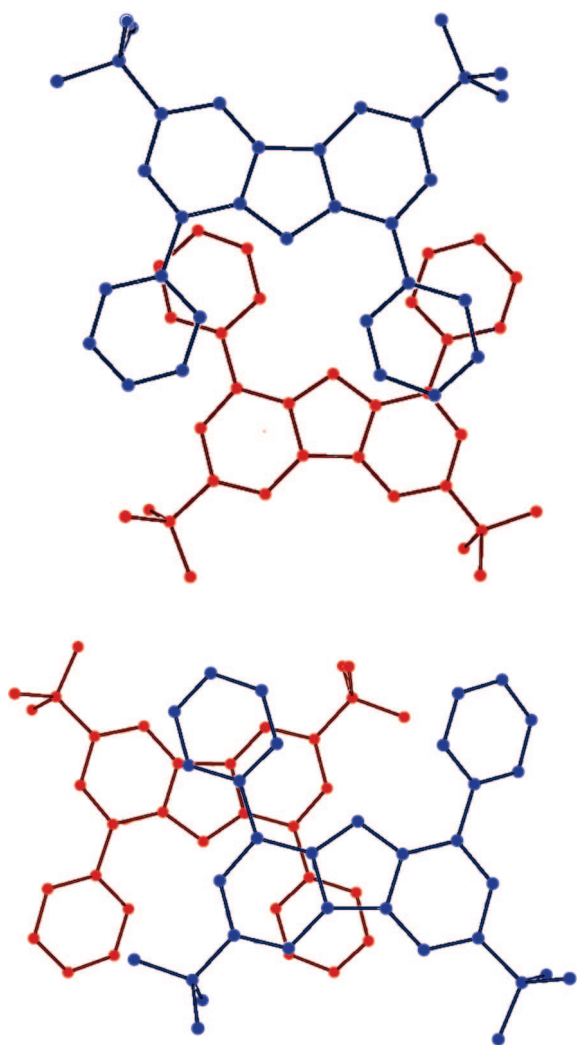


FIGURE 3. Top view showing two molecules of **5H**: type A (top) and type B (bottom).

molecule of the pair causing a larger torsional twist, 18.0° and 22.8° , for this arrangement of **5H**.

Both type A and B molecules have the pyridine nitrogens oriented toward the NH of the central carbazole. The bond lengths for the C–C and C–N bonds in the pyridine and carbazole rings (1.376–1.414 Å) are in the expected range for aromatic systems and no significant bond alternation is observed. The bond connecting the pyridine and carbazole rings is longer

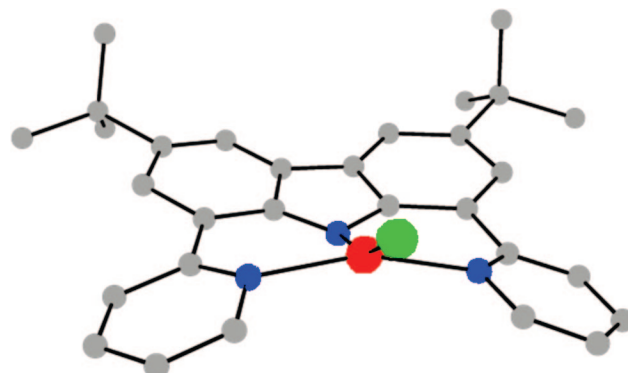


FIGURE 4. Preliminary X-ray structure of $[\text{Pd}(\mathbf{5})\text{Cl}]$ (**20**).

(1.48 Å) as is the central C–C bond of the carbazole (1.45 Å). The N–H of the carbazole is H-bonded to both pyridines with the N–H bond length being 0.88–0.90 Å. The acceptor H---N bond lengths are not exactly equal but differ by about 0.1 Å and the H–N---H bond angle is 114° with one pyridine and 120° with the other for both type A and B molecules.

When the carbazole **5H** is treated with palladium chloride in acetonitrile at reflux the complex **20** is formed in 80% yield. This complex is readily soluble in chloroform and is identified by its ^1H NMR spectrum. Like the free ligand, the complex shows 6 signals in its aromatic region indicating a symmetrical structure. The singlets for H2 and H4 along with the signals for H3'–H5' are only slightly shifted upon complexation. The most characteristic signal is H6' on the two pyridyl rings, which for the free ligand appears as a doublet at 8.90 ppm with a small ($J = 4.2$ Hz) coupling constant. Complexation with Pd(II) shifts this signal down to 10.14 ppm due to charge depletion at the pyridine nitrogens caused by metal binding as well as the deshielding effect of the proximal chlorine. Two attempts to solve the crystal structure for this complex were thwarted by disorder in the crystal lattice. Nevertheless, a reasonable preliminary structure was obtained and is illustrated in Figure 4. The small binding cavity will not accommodate the metal with a planar array of the ligand. The Pd is pushed up out of the plane of the carbazole ring and the chloride is bent even further out of the plane. Attempts to bind other smaller metals in this cavity were unsuccessful.

Spectroscopic Properties

The electronic absorption and emission spectra for the dipyrindylcarbazoles **3H**–**5H** and the palladium complex **20** were recorded in acetonitrile and the data are collected in Table 3. The absorption profiles for the three carbazoles are nearly identical with only a slight difference in energy and absorbance. The dimethyl system gives the lowest energy band at 390 nm, followed by the di-*tert*-butyl at 385 nm and the diprotio at 376 nm.

It is well-known that carbazoles, much like the closely related indoles, are strongly fluorescent. This fluorescence can often be quenched through H-bonding with an appropriate acceptor molecule. In the case of **3H**–**5H** very efficient intramolecular H-bonding exists and so these systems are only very weakly fluorescent with quantum yields of about 4.5×10^{-4} . A detailed study of the excited state proton transfer in **5H** was recently reported.¹⁵ By exposing **5H** to excess D_2O we were able to exchange the N–H proton for deuterium. The resulting stronger N–D bond should proportionately weaken the D---N hydrogen

TABLE 3. Electronic Absorption^a and Emission^b Data for Dipyrildylcarbazoles

compd	λ_{\max} (nm, log ϵ)	λ_{em} (nm)	Φ^c
3H	205 (4.55), 231 (4.67), 295 (4.46), 316 (4.41), 331 (4.23), 362 (4.04), 376 (4.08)	397	4.5×10^{-4}
4H	209 (4.62), 233 (4.77), 297 (4.38), 326 (4.43), 342 (4.26), 376 (4.07), 390 (4.11)	414	4.5×10^{-4}
5H	209 (4.55), 233 (4.72), 298 (4.34), 323 (4.38), 337 (4.22), 370 (4.03), 385 (4.06)	408	4.5×10^{-4}
20	231 (4.50), 283 (4.04), 341 (3.79), 410 (3.71), 451 (3.79)	none	

^a Measured in CH₃CN (10^{-5} M) at room temperature. ^b Measured in CH₃CN (10^{-5} M) at room temperature with excitation at absorbance 0.12. ^c Measured by comparison with data for **5** from ref 4, using quinine sulfate in 0.1 N H₂SO₄ as the standard.

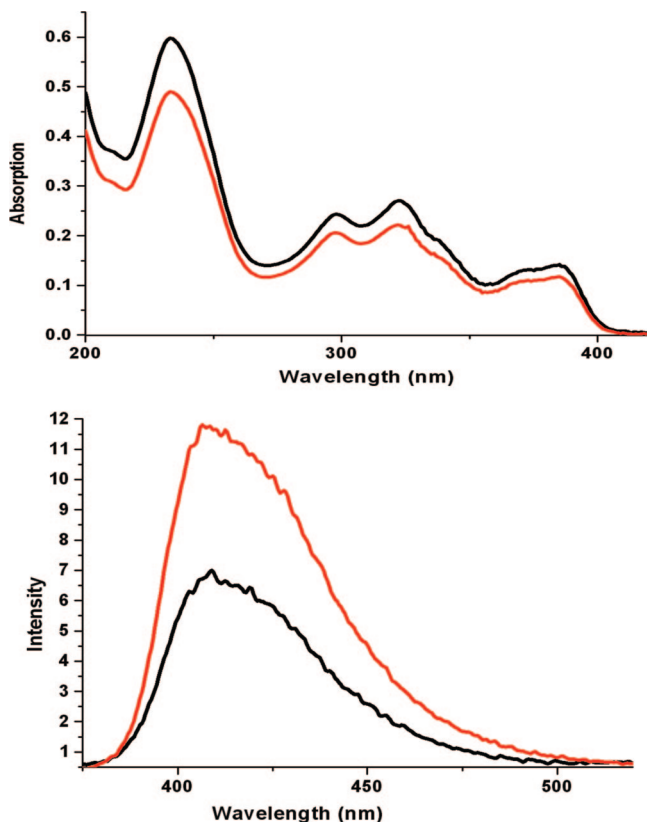


FIGURE 5. Top: Electronic absorption spectra of **5H** (black) and **5D** (red) in CH₃CN (5×10^{-5} M). Bottom: Emission spectra of **5H** (black) and **5D** (red) with excitation at 380 nm. Both taken in CH₃CN (5×10^{-5} M).

bond. Figure 5 shows both the absorption and emission spectra for **5H** and **5D**. While the absorption spectra are nearly superimposable, the emission spectrum for the deuterated carbazole is considerably more intense, indicating that the quenching process is less efficient for this species.

In somewhat related work we and others have examined polypyridine-type complexes of Pt(II)¹⁶ and Ru(II)¹⁷ complexes in which the metal is contained in a six-membered rather than a five-membered chelate ring. The ligands were designed so as to maintain complete conjugation of the aromatic system. In both cases the six-membered chelate ring provided a less strained coordination environment leading to a more stable ligand field. This, in turn, resulted in less nonradiative decay of the excited

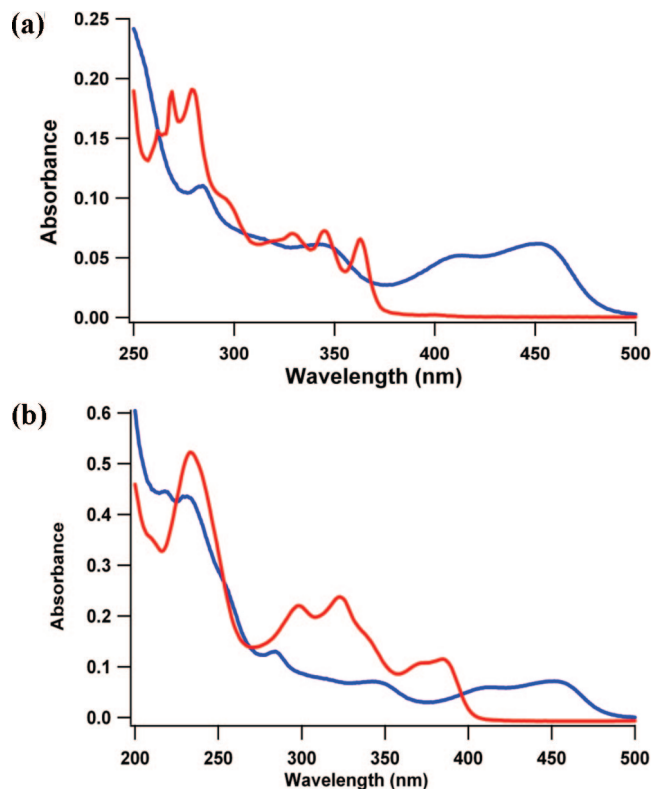


FIGURE 6. (a) Top: Electronic absorption spectra of [Pd(tpy)Cl]Cl (red) and **20** (blue) in CH₃CN (5×10^{-5} M). (b) Bottom: Electronic absorption spectra of **5H** and **20** in CH₃CN (5×10^{-5} M).

state and a more intense luminescence at room temperature. The Pd complex **20** contains two fused six-membered chelate rings and thus might be expected to enjoy some of the same enhancements of its ligand field.

The absorption spectrum of **20** is shown in Figure 6a compared with the spectrum of [Pd(tpy)Cl]Cl where tpy = 2,2';6,2''-terpyridine. While the absorbance of [Pd(tpy)Cl]Cl falls off sharply beyond 370 nm, the complex **20** shows two broad bands centered at 410 and 451 nm. Bands in this region are often assigned to metal-to-ligand charge transfer; however, in this case, such an assignment is highly unlikely. The Pd^{II} potential is too high to make this state easily accessible and furthermore the anionic ligand would be a very poor charge acceptor. A more reasonable explanation would involve intraligand charge transfer from the carbazole as donor to the pyridine as acceptor. This assignment is strengthened by the observation in Figure 6b that similar absorption bands at 370 and 385 nm appear for the free ligand **5H** and are red-shifted upon complexation to Pd(II).

The solid state IR spectra of the complexes were measured and found to be consistent with the other spectroscopic evidence. Figure 7 illustrates the IR spectra of **3H**–**5H** as well as that of the deuterio-derivative **5D**. For the parent carbazole **3H** the

(15) Wiosna-Salyga, G.; Dobkowski, J.; Mudadu, M.; Sazanovich, I.; Thummel, R. P.; Waluk, J. *Chem. Phys. Lett.* **2006**, *423*, 288–292.

(16) Hu, Y.-Z.; Wilson, M. H.; Zong, R.; Bonnefous, C.; McMillin, D. R.; Thummel, R. P. *Dalton Trans.* **2005**, 354–358.

(17) (a) Abrahamsson, M.; Jäger, M.; Osterman, T.; Eriksson, L.; Persson, P.; Becker, H. C.; Johansson, O.; Hammarström, L. *J. Am. Chem. Soc.* **2006**, *128*, 12616–12617. (b) Abrahamsson, M.; Becker, H. C.; Hammarström, L.; Bonnefous, C.; Chamchoumis, C.; Thummel, R. P. *Inorg. Chem.* **2007**, *46*, 10354–10364.

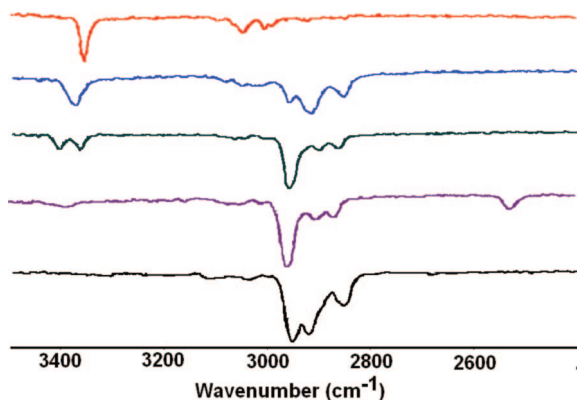


FIGURE 7. Solid state IR spectra taken at 25 °C: **3H** (red), **4H** (blue), **5H** (green), **5D** (purple), and **20** (black).

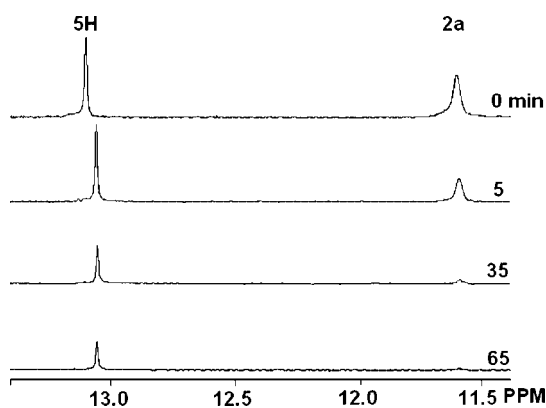


FIGURE 8. D₂O exchange competition between **2a** and **5H** as monitored by ¹H NMR. Spectra show the NH resonances for a 1:1 mixture of **2a** and **5H**. The top spectrum is before the addition of D₂O and the successive spectra are at time intervals of 5, 35, and 65 min.

prominent peak at 3354 cm⁻¹ is associated with the N–H stretch. In the dimethyl derivative **4H** this absorption broadens and moves to 3375 cm⁻¹ while characteristic C–H bands appear in the region around 2900 cm⁻¹. For the di-*tert*-butyl derivative **5H** the N–H band splits into two peaks at 3364 and 3405 cm⁻¹, which is consistent with the existence of two molecules, type A and type B, in the solid state structure of this species. For this molecule the C–H absorption at 2960 cm⁻¹ becomes more significant. Finally, the deuterated derivative of **5H** shows almost complete disappearance of the two N–H stretching bands and the appearance of a much weaker single band at an intermediate frequency of about 3376 cm⁻¹. At the same time a new peak appears at 2528 cm⁻¹, which is expected for the N–D stretch. It is possible that upon deuteration the morphology of the solid state of **5D** changes to a single type of molecule rather than the type A and type B which were observed for **5H**. The IR spectrum of the Pd complex **20** shows the same typical C–H stretching bands and the clear absence of the N–H stretch.

To compare the H-bonding in **5H** with that of **2a**, a competition exchange experiment was carried out involving these two species. The top spectrum in Figure 8 shows the NH resonances for an equimolar (0.005 mmol) solution of these two compounds in CDCl₃. Already some interesting features are evident. For the carbazole **5H**, having a bifurcated H-bond, the NH resonance appears at much lower field due to the stronger deshielding effect of the “double” H-bond. Notice also that this peak is sharper, indicating less motion of the proton. Upon the addition of D₂O (0.025 mmol) the NH peak for **2a** disappears

more rapidly indicating a faster exchange of this proton. After 65 min all of **2a** has exchanged while approximately 25% of **5H** remains as the unexchanged protio species.

Conclusions

A series of three 1,8-di(pyridin-2'-yl)carbazoles was prepared by Stille coupling of the appropriate dibromocarbazole precursors. These precursors are prepared by three different approaches. A crystal structure of **5H** indicates that the carbazole NH is H-bonded to both pyridine rings, leading to a syn coplanar arrangement of the molecule, which crystallizes in two different forms. The absorption spectra evidence what appears to be an intraligand charge transfer from the carbazole to the pyridines. The strong intramolecular H-bond effectively quenches excited state emission and significantly slows down D–H exchange. The binding cavity in these dipyridocarbazoles is small but Pd can be accommodated by out-of-plane twisting of the peripheral pyridine rings.

Experimental Section

3,6-Dinitrocarbazole (7). A three-necked round-bottomed flask, equipped with condenser, addition funnel, and stirring bar, was charged with carbazole (10.03 g, 60.0 mmol) and glacial AcOH (80 g) under Ar. The mixture was stirred for 1.5 h at 40 °C. Then, 10% HNO₃/AcOH (1:1, 16.4 g) was added dropwise and the mixture was stirred for 2 h at 90–100 °C. The yellow precipitate was filtered and washed with cold AcOH (50 mL) and then with water. The solid was warmed in KOH/EtOH (200 mL, 60 g/L) at 50 °C for 30 min and filtered. The insoluble red solid was digested in 10% HCl at 100 °C for 2 h. The resulting yellow solid was filtered, washed with water, and dried overnight under vacuum in the presence of P₂O₅. Chromatography on alumina, eluting with CH₂Cl₂, followed by AcOEt and MeOH, provided **7** (5.25 g, 34%): mp >300 °C (lit.⁶ mp 386–387 °C); ¹H NMR (DMSO-*d*₆) δ 12.73 (br s, 1H), 9.47 (d, 2H, *J* = 2.1 Hz), 8.36 (dd, 2H, *J* = 9.3, 2.7 Hz), 7.74 (d, 2H, *J* = 9.0 Hz).

1,8-Dibromo-3,6-dinitrocarbazole (10). A mixture of 4,7-dinitrocarbazole (**7**, 0.23 g, 0.9 mmol), bromine (0.5 mL, 1.5 mmol), and H₂SO₄ (6 mL) was warmed for 15 min at 90–100 °C. Then, additional bromine (0.3 mL, 0.9 mmol) and H₂SO₄ (6 mL) were added. The resulting mixture was heated at 100 °C for 2.5 h. After cooling to room temperature the brown reaction mixture was poured onto ice and filtered to provide **10** (0.37 g, 99%) as a yellow-green solid: mp >300 °C (lit.⁷ mp >320 °C); ¹H NMR (DMSO-*d*₆) δ 12.80 (br s, 1H), 9.54 (d, 2H, *J* = 2.7 Hz), 8.56 (d, 2H, *J* = 1.8 Hz).

3,6-Diamino-1,8-dibromocarbazole (11). A mixture of 1,8-dibromo-3,6-dinitrocarbazole (**10**, 0.33 g, 0.8 mmol), iron powder (0.89 g, 16.0 mmol), and concentrated HCl (1.53 g, 16.0 mmol) in EtOH/H₂O (3:1, 100 mL) was mechanically stirred at reflux for 19 h. After cooling, the reaction mixture was filtered and the solvent evaporated. The aqueous residue was made alkaline with 10% NaOH and extracted with THF/AcOEt (1:1, 3 × 100 mL). The combined organic phase was washed with brine (20 mL), dried (MgSO₄), and concentrated to provide **11** as a yellowish solid (0.18 g, 65%): mp 238–240 °C dec; ¹H NMR (DMSO-*d*₆) δ 9.79 (s, 1H), 7.03 (s, 2H), 6.94 (s, 2H), 4.95 (br s, 4H); ¹³C NMR (DMSO-*d*₆) δ 142.8, 132.0, 125.5, 117.3, 104.1, 103.2; HRMS *m/z* calcd for C₁₂H₆Br₂N₃ [M⁺] 352.9163, found 352.9159.

1,8-Dibromocarbazole (12).^{8b} A solution of water (1.2 mL) and concentrated HCl (0.5 mL) was heated to reflux. The heat was removed and 3,6-diamino-1,8-dibromocarbazole (**11**, 0.15 g, 0.4 mmol) was added. EtOH (1 mL) was added to help dissolution of the solid. The mixture was refluxed for 45 min. The solution was allowed to cool to 15 °C in an ice bath and more HCl (0.2 mL)

was added. When the temperature reached 10–13 °C, a solution of NaNO₂ (0.7 g, 1.0 mL) in H₂O (1 mL) was added dropwise. The yellow mixture was stirred for 30 min at 5–10 °C. Then cold 50% H₃PO₂ (1.0 mL) was added. The mixture was stoppered loosely and kept in the refrigerator for 11 h. Then the reaction mixture was stirred at room temperature for 24 h. The EtOH was evaporated and the residue was dissolved in CH₂Cl₂. The two layers were separated and the aqueous phase was extracted with CH₂Cl₂ (3 × 20 mL). The combined organic phase was washed with brine (20 mL), dried (MgSO₄), and concentrated to provide **12** as a yellowish solid (0.09 g, 70%): mp 110–12 °C; ¹H NMR (DMSO-*d*₆) δ 11.18 (br s, 1H), 8.18 (d, 2H, *J* = 7.8 Hz), 7.66 (d, 2H, *J* = 7.8 Hz), 7.17 (t, 2H, *J* = 7.8 Hz); ¹H NMR (CDCl₃) δ 8.27 (br s, 1H), 7.92 (d, 2H, *J* = 8.1 Hz), 7.57 (d, 2H, *J* = 7.83 Hz); ¹³C NMR (CDCl₃) 137.6, 128.68, 124.7, 121.1, 119.7, 104.4; HRMS *m/z* calcd for C₁₂H₇Br₂N [M⁺] 322.8945, found 322.8940.

3,6-Dimethylcarbazole (14). A mixture of di-*p*-tolylamine (0.39 g, 2.0 mmol), palladium(II) diacetate (0.45 g, 2.0 mmol), and glacial AcOH (40 mL) was refluxed for 1.5 h in the presence of atmospheric oxygen.¹¹ After cooling to room temperature, the mixture was concentrated. The red residue was dissolved in CH₂Cl₂ and filtered through Celite. The organic solution was washed with brine (20 mL), dried (MgSO₄), and concentrated. Chromatography on alumina, eluting with CH₂Cl₂/petroleum ether provided **14** (0.19 g, 53%) as a white solid: mp 215–217 °C (lit.^{12c} mp 219–220 °C); ¹H NMR (acetone-*d*₆) δ 10.08 (br s, 1H), 7.86 (d, 2H, *J* = 0.9 Hz), 7.36 (d, 2H, *J* = 8.1 Hz), 7.19 (d, 2H, *J* = 8.4 Hz), 2.48 (s, 6H).

1,8-Dibromo-3,6-dimethylcarbazole (15).¹² To a warm (90 °C) solution of 3,6-dimethylcarbazole (**14**, 0.40 g, 2.2 mmol) in glacial AcOH (87 mL) was added a solution of bromine (0.73 g, 4.6 mmol) in AcOH (6 mL) in one portion. The mixture was stirred at 90 °C under Ar for 3.5 h. After cooling to room temperature, the reaction mixture was concentrated and dried. The solid obtained was washed with hexane, filtered, and dried to provide **15** as a white solid (0.28 g, 37%): mp 192–193 °C; ¹H NMR (acetone-*d*₆) δ 10.16 (br s, 1H), 8.56 (s, 2H), 7.60 (s, 2H), 2.52 (s, 6H). This material was used in the subsequent Stille coupling step without further purification.

1,3,6,8-Tetra(tert-butyl)carbazole (16), 3,6-Di(tert-butyl)carbazole (17), and 1,3,6-Tri(tert-butyl)carbazole (18).¹³ To a suspension of carbazole (2.90 g, 17.4 mmol) and freshly distilled 2-chloro-2-methylpropane (9.65 g, 104.2 mmol) was added AlCl₃ (2.32 g, 17.4 mmol) during 1 h. Concentrated HCl (50 mL) was added and the mixture was stirred at room temperature for 24 h. Then, ice–water was added. The mixture was extracted with Et₂O (3 × 50 mL). The aqueous phase was concentrated to a smaller volume and extracted with Et₂O (3 × 40 mL). The combined organic phase was washed with brine (20 mL), dried (MgSO₄), and concentrated. Chromatography on silica gel, eluting with benzene/hexane (1:1) provided **16** (2.09 g, 30%), **17** (1.15 g, 24%), and **18** (1.04 g, 18%) as white solids. **16**: mp 189 °C (lit.¹³ mp 191–192 °C); ¹H NMR (CDCl₃) δ 8.14 (br s, 1H), 7.95 (d, 2H, *J* = 1.5 Hz), 7.46 (d, 2H, *J* = 2.4 Hz), 1.60 (s, 18H), 1.46 (s, 18H). **17**: mp 212 °C (lit.¹³ mp 228–229 °C); ¹H NMR (CDCl₃) δ 8.08 (d, 2H, *J* = 1.2 Hz), 7.46 (dd, 2H, *J* = 8.7, 2.4 Hz), 7.34 (d, 2H, *J* = 8.7 Hz), 1.44 (s, 18H). **18**: mp 134–136 °C (lit.¹³ mp 136–137 °C); ¹H NMR (CDCl₃) δ 8.07 (d, 1H, *J* = 1.8 Hz), 7.96 (d, 1H, *J* = 2.1 Hz), 7.47 (dd, 1H, *J* = 8.4, 1.8 Hz), 7.42 (d, 1H, *J* = 1.5 Hz), 7.37 (d, 1H, *J* = 8.4 Hz), 1.57 (s, 9H), 1.46 (s, 9H), 1.45 (s, 9H).

3,6-Di(tert-butyl)carbazole (17).¹³ A mixture of **16** (1.53 g, 3.9 mmol) and concentrated H₂SO₄ (30 mL) was stirred at room temperature for 24 h. Ice water (200 mL) was added, and the mixture was extracted with AcOEt (5 × 50 mL). The combined organic phase was washed with water (20 mL) and brine (20 mL), dried (MgSO₄), and concentrated. Chromatography on silica gel, eluting with benzene/hexane (1:1) provided **17** (0.63 g, 58%), which was identical with the material obtained from the direct alkylation of carbazole.

1,8-Dibromo-3,6-di(tert-butyl)carbazole (19).¹⁴ In the manner described for **15**, a mixture of 3,6-di(tert-butyl)carbazole (**18**, 0.81 g, 2.9 mmol), bromine (0.96 g, 6.0 mmol), and glacial AcOH (128 mL) gave a crude product, which after chromatography on silica gel, eluting with CH₂Cl₂, provided **19** (0.98 g, 77%) as a white solid: mp 174–175 °C (lit.¹⁴ mp 171–172 °C); ¹H NMR (CDCl₃) δ 8.14 (br s, 1H), 7.97 (d, 2H, *J* = 1.2 Hz), 7.64 (d, 2H, *J* = 1.8 Hz), 1.43 (s, 18H).

1,8-Di(pyrid-2'-yl)carbazole (3H). A two-necked round-bottomed flask, equipped with a magnetic stir bar, condenser, and rubber septum, was charged with 1,8-dibromocarbazole (**12**, 72.0 mg, 0.23 mmol), 2-(tri-*n*-butylstannyl)pyridine (85%, 238.0 mg, 0.55 mmol), tetrakis(triphenylphosphine)palladium(0) (5% mol, 23.1 mg, 0.02 mmol), and dry toluene (2 mL) was refluxed under Ar for 20 h. After cooling to room temperature, water (1 mL) was added and the mixture was concentrated under reduced pressure. Chromatography on silica gel, eluting with CH₂Cl₂ provided **3** (53.0 mg, 27%) as a white solid, which was recrystallized from CH₂Cl₂/hexane: mp 215–217 °C; ¹H NMR (DMSO-*d*₆) δ 13.54 (br s, 1H), 9.01 (d, 2H, *J* = 3.6 Hz), 8.30 (t, 4H, *J* = 7.5 Hz), 8.19 (d, 2H, *J* = 7.2 Hz), 7.99 (td, 2H, *J* = 5.7, 1.8 Hz), 7.45 (dd, 2H, *J* = 6.9, 4.8 Hz), 7.36 (d, 1H, *J* = 7.8 Hz); ¹H NMR (CDCl₃) δ 13.54 (br s, 1H), 8.93 (dd, 2H, *J* = 4.2, 1.5 Hz), 8.22 (d, 2H, *J* = 7.8 Hz), 8.06 (d, 2H, *J* = 8.4 Hz), 8.00 (d, 2H, *J* = 7.8 Hz), 7.85 (td, 2H, *J* = 7.85, 1.8 Hz), 7.35 (t, 2H, *J* = 7.8 Hz), 7.30 (dd, 1H, *J* = 7.5, 5.1 Hz); ¹³C NMR (CDCl₃) δ 157.4, 148.7, 138.4, 136.9, 124.2, 123.5, 121.6, 121.4, 120.6, 120.4, 118.9; HRMS *m/z* calcd for C₂₂H₁₅N₃ [M + H] 322.1344, found 322.1345.

1,8-Di(pyrid-2'-yl)-3,6-dimethylcarbazole (4H). In the manner described for **3H**, a mixture of 1,8-dibromo-3,6-dimethylcarbazole (**15**, 0.53 g, 1.5 mmol), 2-(tri-*n*-butylstannyl)pyridine (85%, 1.56 g, 3.6 mmol), and tetrakis(triphenylphosphine) palladium(0) (92.0 mg, 0.08 mmol) in dry toluene (12 mL) was refluxed under Ar. After 24 h, more 2-(tri-*n*-butylstannyl)pyridine (0.22 g, 0.5 mmol) was added and the reaction mixture was refluxed for a further 17 h. After cooling to room temperature, water (1 mL) was added and the mixture was concentrated under reduced pressure. Chromatography on alumina, eluting with CH₂Cl₂/hexane (1:1) provided a solid, which was washed with Et₂O, filtered, and dried to provide **4** as a yellow solid (0.09 g, 17%): mp 242–243 °C; ¹H NMR (CDCl₃) δ 12.98 (br s, 1H), 8.89 (d, 2H, *J* = 3.9 Hz), 8.03 (d, 2H, *J* = 8.1 Hz), 7.96 (s, 2H), 7.81 (t, 2H, *J* = 7.5 Hz), 7.78 (s, 2H), 7.25 (t, 2H, *J* = 6.0 Hz), 2.62 (s, 6H); ¹³C NMR (acetone-*d*₆) δ 158.4, 150.0, 137.9, 137.8, 128.7, 125.5, 125.1, 122.6, 122.5, 121.3, 120.9, 21.7; HRMS *m/z* calcd for C₂₄H₁₉N₃ [M + H] 350.1657, found 350.1656.

1,8-Di(pyrid-2'-yl)-3,6-di(tert-butyl)carbazole (5H). In the manner described for **3H**, a mixture of 1,8-dibromo-3,6-di(tert-butyl)carbazole (**19**, 0.51 g, 1.2 mmol), 2-(tri-*n*-butylstannyl)pyridine (85%, 1.66 g, 3.8 mmol), and tetrakis(triphenylphosphine)palladium(0) (69.3 mg, 0.06 mmol) in dry toluene (4 mL) provided a crude material. Chromatography on alumina, eluting with AcOEt/hexane (1:4) provided impure **5**. A second chromatography on alumina, eluting with hexane, then CH₂Cl₂/hexane (1:1) provided **5** (0.38 g, 74%) as a white solid, which was recrystallized from CH₂Cl₂/hexane: mp 255–256 °C; ¹H NMR (CDCl₃) δ 12.88 (br s, 1H), 8.90 (dd, 2H, *J* = 3.9, 0.8 Hz), 8.23 (d, 2H, *J* = 1.2 Hz), 8.06 (d, 2H, *J* = 7.8 Hz), 8.02 (d, 2H, *J* = 1.5 Hz), 7.83 (td, 2H, *J* = 8.1, 2.1 Hz), 7.25 (m, 2H) 1.54 (s, 18H); ¹³C NMR (CDCl₃) δ 158.3, 149.1, 141.6, 137.3, 136.7, 124.3, 121.3, 121.2, 120.4, 118.0, 35.0, 32.4 (one carbon hidden). Anal. Calcd for C₃₀H₃₁N₃: C, 83.14; H, 7.16; N, 9.70. Found: C, 83.05; H, 7.33; N, 9.67.

[(5)PdCl] (20). A mixture of **5H** (50 mg, 0.109 mmol) and PdCl₄K₂ (40 mg, 0.109 mmol) in MeCN (10 mL) was refluxed under Ar for 24 h. The solvent was evaporated under reduced pressure. Chromatography on silica gel, eluting with acetone/hexane (2:1) gave **20** as a brown solid (0.050 g, 80%): ¹H NMR (CDCl₃) δ 10.14 (d, 2H, *J* = 6.0 Hz), 8.27 (s, 2H), 8.23 (d, 2H, *J* = 8.7 Hz), 7.95–7.90 (t, 2H, *J* = 7.8 Hz), 7.92 (s, 2H), 7.28–7.24 (t,

2H, $J = 8.4$ Hz), 1.62 (s, 18H); ^{13}C NMR (CDCl_3) δ 155.9, 152.1, 141.7, 139.9, 138.1, 126.4, 122.2, 122.0, 121.3, 120.5, 119.8, 34.9, 32.1; HRMS m/z calcd for $\text{C}_{30}\text{H}_{30}\text{N}_3\text{ClPd} [\text{M} - \text{Cl}]^+$ 538.1474, found 538.1485.

Acknowledgement. We thank the Robert A. Welch Foundation (E-621) and the National Science Foundation (CHE-0352617) for financial support. We would also like to thank Dr. James Korp for assistance with the X-ray determinations and Professor Sebastiano Campagna for helpful discussions.

Supporting Information Available: General Experimental Methods; X-ray analysis of **5H**, Table S1 giving data collection and processing parameters for **5H**, ^1H and ^{13}C NMR spectra for **3H–5H**, **11**, **12**, and **20**, ^1H NMR for **7**, **10**, and **14–19**, and X-ray crystallographic data (CIF files) for **5H**. This material is available free of charge via the Internet at <http://pubs.acs.org>.

JO801132W